HENRY

Hydraulic Engineering Repository

Ein Service der Bundesanstalt für Wasserbau

Conference Paper, Published Version

Bel, Coraline; Jodeau, Magali; Tassi, Pablo; Claude, Nicolas; Haddad, Hanna

Calibration and validation strategy for 2D hydrodynamic modelling: application to morphodynamics of a gravel-bed river with suspended sediments

Calibration and validation strategy for 2D hydrodynamic modelling: application to morphodynamics of a gravel-bed river with suspended sediments

Coraline Bel (1), Magali Jodeau (1, 2), Pablo Tassi (1,2)

(1): Saint-Venant Hydraulics Laboratory (LHSV)
ENPC, Cerema, EDF R&D
Chatou, France
coraline.bel@enpc.fr

Nicolas Claude (2), Hanna Haddad (2)

(2): National Hydraulics and Environment Laboratory (LNHE)
EDF R&D
Chatou, France

Abstract—**This work aims at presenting an example of application of the APIs for the step of hydrodynamic model calibration and validation in the case of an ongoing study. The study site is a gravel bed river where the fine sediment dynamics is a main concern of the river management.**

I. INTRODUCTION

Nowadays, many mountain and piedmont regulated rivers present steady vegetated alternate bar systems as a consequence of the anthropogenic modifications – embankment, hydroelectric facilities, gravel extraction, land use change, etc. – that, over the last two centuries, have impacted the hydrologic regime and the sediment supply [1]. During high flow events, massive deposits of fine sediment occur on gravel bars, leading to bar elevation, riparian vegetation growth and consequently to bar stabilization (Fig. 1). This results in river ecological quality degradation and increased flooding risk. To optimize gravel-bed river management strategies aiming at preventing bar colonization by plants, a better understanding of the involved processes is necessary. In particular, improving our knowledge of cohesive sediment dynamics (storage and re-suspension) on gravel bars during varying hydrologic events (natural flood and reservoir flushing) is important. The purpose of our study is to investigate hydro-morphodynamic processes at the scale of a few kilometers long reach, by means of flow and sediment transport simulations performed using the modules TELEMAC-2D and GAIA [2] (previously SISYPHE) of the TELEMAC-MASCARET suite of solvers. The implemented two-dimensional (2D) model accounts for bedload and suspended load transport processes of cohesive and non-cohesive sediments.

The study site is the Combe-de-Savoie reach of the Isère River (France). A field campaign performed in 2018 during a reservoir flushing event showed that both bedload and mixed (cohesive and non-cohesive) suspended sediment transport play a critical role on the morphological evolution of the riverbed. In this study case, accounting for bedload transport processes is important to capture significant bathymetric changes, while modelling suspended load transport is necessary to reproduce distribution and thickness of fine sediment deposits, for both sands and cohesive sediments.

Before examining the effects of different environmental forcing (e.g., water and sediment supplies, etc.) on bed evolution to propose new management strategies, the numerical model must be calibrated and validated. This is done in two consecutive steps, according to the different physical processes: (i) the calibration and validation of the hydrodynamics, and (ii) the calibration and validation of the sediment transport and morphodynamics. Here, we will focus on the former step.

The calibration and validation procedure of the hydrodynamic model is supported by high-quality water surface elevation and flow velocity measurements. This proceeding aims to detail the strategy adopted for the optimal and efficient parametrization of the hydrodynamic model. For this purpose, the APIs (Application Programming Interface) developed for the automatic model calibration using data assimilation algorithm [3], [4] are used.
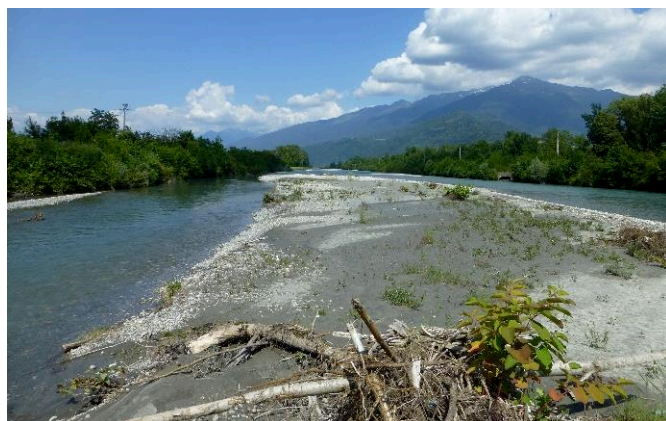

Figure 1. *Example of fine deposit and vegetation establishment on gravel bar. Fréterive gravel bar, June 2018.*

II. STUDY CASE

A. Study site

The Isère River is an Alpine regulated gravel-bed river located in South-Eastern France. Its flood regime is pluvio-nival and impacted by hydroelectric structures. The study reach is located downstream the Aigueblanche reservoir dam, in the Fréterive area at Combe-de-Savoie, southwest of Albertville (Fig. 2). It is about 100-m wide between dikes, and extends over 3 km up to upstream of the Arc-Isère confluence. The bed slope is 0.0016 m/m. The D_{50} is approx. 24 mm, 180 µm, and 50 µm for coarse, non-cohesive (2-0.063 mm) and cohesive (<0.063 mm) sediments respectively. In this area, the flow discharges for 2 and 10-year floods are 209 m³/s and 345 m³/s, respectively. The average suspended sediment concentration (SSC) is less than 1 g/l but can reach up to about 10 g/l during major floods.

In winter 2017, this area was the subject to restoration works which consisted in removing fine sediment and vegetation, and in remodelling a part of the bared gravel bars.
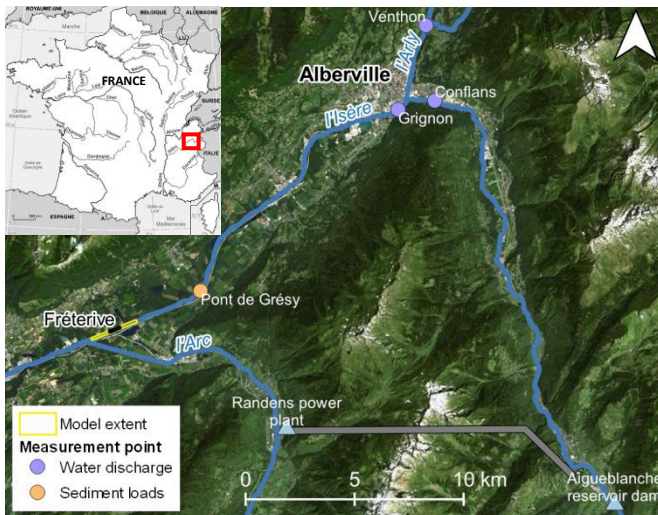

Figure 2. *Study site map and extent of the model: Isère River at Combe-de-Savoie.*

B. Field data

In 2018, time series of water discharge, suspended sediment concentration (both cohesive sediment and sand) were reconstructed upstream the study reach, at Pont-de-Grésy, with a 1-h time step from January 1 to September 28 (Figs. 2 and 3). Similarly, bedload fluxes (estimated with a hydrophone [5]) were reconstructed from March 21 to June 7. During the same period, free surface elevation was also recorded using four piezometers distributed along a part of the study reach, in the area of Fréterive (Fig. 7).

From May 6 to 11 2018, a comprehensive field campaign was conducted during the reservoir flushing of the Aigueblanche dam (Fig. 2). During the flushing event, point measurements of current velocities (aDcp – Fig. 7), of fine sediment settling velocities (SCAF measurements on SSC samples at Pont-de-Grésy [6], [7]), of bedload fluxes and of grain size of the transported fraction (Helley-Smith samples

at Pont-de-Grésy, etc.) were performed. In addition, pre- and post-event measurements were achieved, in particular on the Fréterive gravel bar, including aerial photographies, topo-bathymetry (Fig. 5), flow velocities (LSPIV [8] – Figs. 4 and 7), gravel-bar material characterisation (measurements of grain size by mass on cryogenic coring, and by Wolman pebble count technic on bars – Fig. 6), fine-sediment deposit
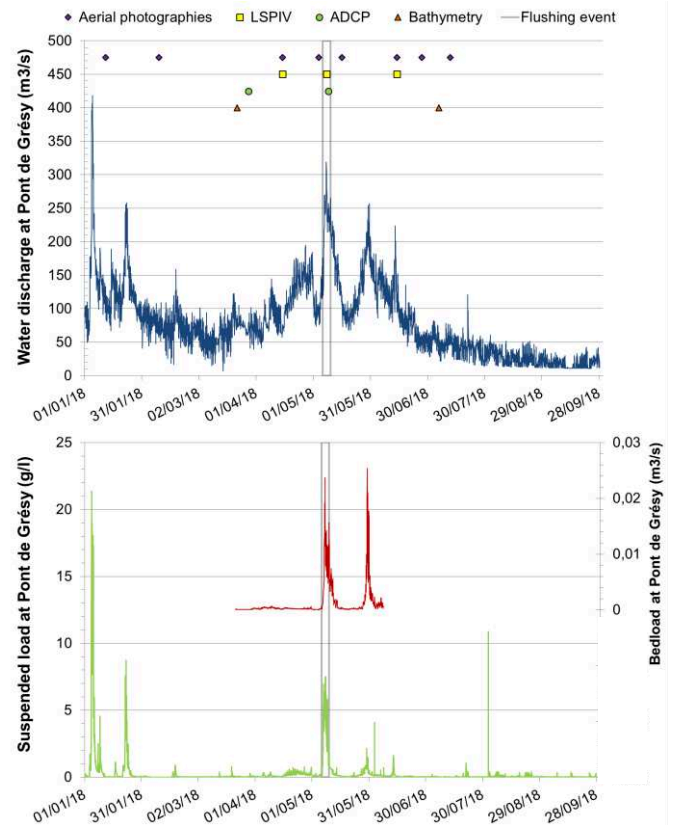

Figure 3. *Dates of the surveys, time series of water discharge(blue), suspended load (green) and bedlaod (red) recorded at Combe-de-Savoie.*
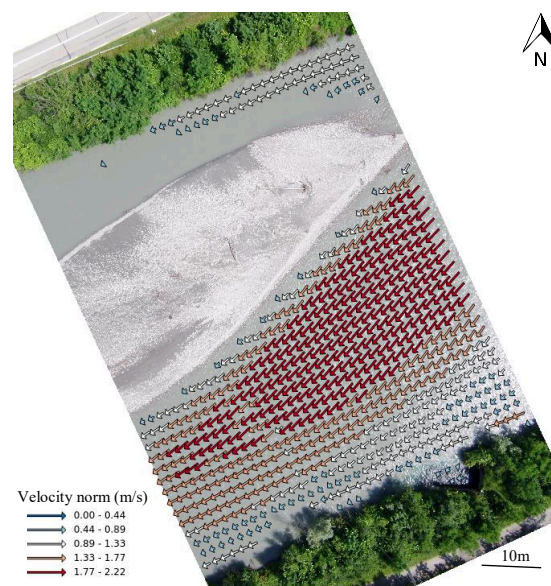

Figure 4. *Extract of velocities field obtained by LSPIV on June 14,2018.*

characterisation, geomorphic observations and vegetation monitoring.

All these measurements are used either as model input, as prior knowledge of model parameters, or again as comparison elements for the calibration and validation stages.

Before going further in the numerical model, few elements of analysis of the measurements may be introduced. The comparison of the bathymetric surveys before and after the flushing event shows significant changes (Fig. 5). It emphasises the importance of anticipating the bed modification while ajusting the hydrodynamic parameters in the former step of modelling. It also bring out the key role played by bedload transport which must be represented in the morphodynamic modelling. The grain size measurements, by mass or by counting, at the surface of gravel bars (Fig. 6) are consistent and highlights the strong heterogenity present in
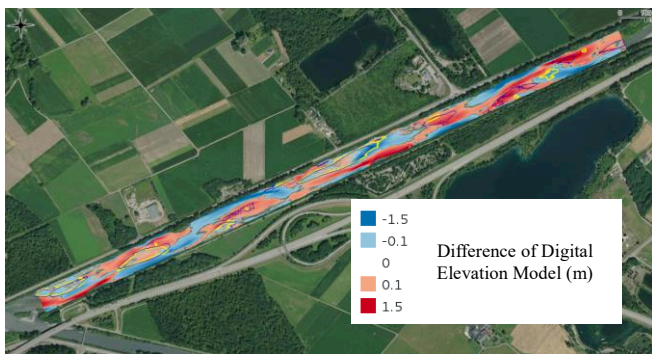

Figure 5. *Bathymetric evolution from March to July 2018.The limits of flooded areas before (04/05/2018) and after (16/05/2018) the flushing event are marked with the yellow and blue lines.*
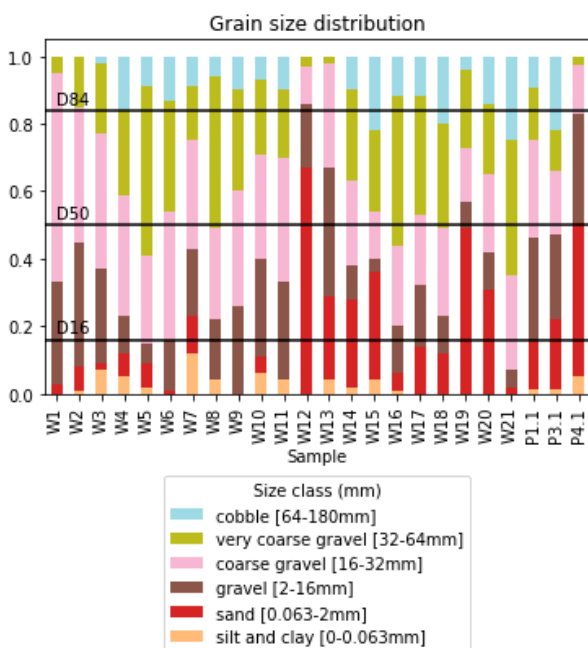

Figure 6. *Grain size distribution at bar surface. Wx: Wolman pebble count on bars; Px.1: mass grain size on 0-20cm layer of cryogenic cores.*

field environnement (Fig. 1). Even so, the D_{50} may be represented by coarse gravel. Otherwise, we can notice the important proportion of cohesive sediments and sand, and so the necessity of properly representing the suspended load in the morphodynamic modelling.

III. NUMERICAL MODEL

A. Mesh and boundary conditions

The computational domain extent starts downstream Pont-de-Gresy and stops upstream the confluence with the Arc River so that the confluence with Arc is not modelled. The flow regime is subcritical and there is no flow change. The upstream boundary condition is a prescribed flow rate based on the Pont-de-Grésy records. The downstream boundary condition is a prescribed elevation that is function of the discharge, on the basis of a stage-discharge relationship established at the level of the fourth piezometer. Two different friction areas are defined to separate the main stream from the vegetated banks. No friction area is dedicated to the bars (tidal flats) although the friction coefficient may differ from the main stream because of logjam and young vegetation (Fig. 1). This choice is made because the limits of these areas may evolve due to bed modification (Fig. 5) and so fixing these areas could generate a modelling artefact during the morphodynamic simulation.

The model consists of an unstructured mesh discretized with 117,557 triangular elements (approximately 60,000 nodes) with a 2-m resolution (Fig. 6). A mesh convergence analysis was performed based on several mesh refinements, ranging from 8 to 0.5-m resolution using the STBTEL module.
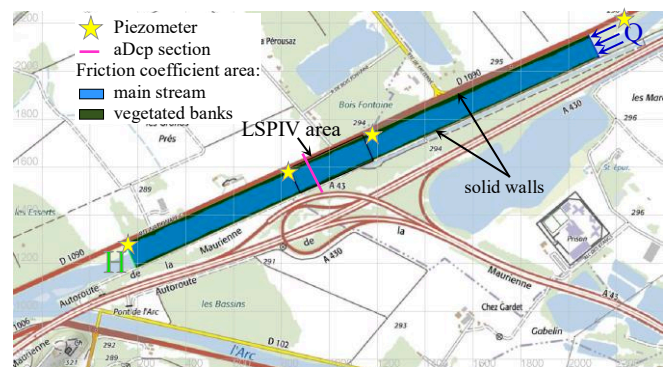
Figure 7. *Mesh and boundary conditions of the hydrodymanic model. Piezometer position. LSPIV area and aDcp section.*

B. Equations and parameters to calibrated

In this study, flow, sediment transport and bed evolution are simulated by coupling the modules TELEMAC-2D and GAIA so as to solve, at each time step, (i) the hydrodynamics with fixed bottom [9], then (ii) the morphodynamics [10]. In this section, we focus on the hydrodynamic modelling.

Hereafter, the unknowns, the variables requiring a closure model and the calibration parameters are noted in red, in blue and in green respectively.

TELEMAC-2D solves the non-conservative shallow-water equations (1) and requires one closure model for friction and one closure model for turbulence.

$$\begin{cases} \partial_t h + \boldsymbol{u} \cdot \mathbf{grad}(h) + h \, \mathrm{div}(\boldsymbol{u}) = 0 \\ \partial_t u + \boldsymbol{u} \cdot \mathbf{grad}(u) = -g \, \partial_x z_s + F_x^f + \frac{1}{h} \mathrm{div}\big(h \, \nu_t \, \mathbf{grad}(u)\big) \\ \partial_t v + \boldsymbol{u} \cdot \mathbf{grad}(v) = -g \, \partial_y z_s + F_y^f + \frac{1}{h} \mathrm{div}\big(h \, \nu_t \, \mathbf{grad}(v)\big) \end{cases} \quad (1)$$

with h (m) the water level, u,v (m/s) the horizontal velocity components, $z_s = z_b + h$ (m) the free surface elevation, z_b (m) the bottom elevation, g (m/s²) the gravity acceleration, t (s) the time, and x,y (m) the horizontal space coordinates.

$\left(F_x^f, F_y^f\right) = f(\boldsymbol{u}, h, k_s)$ (m/s²) are the friction source terms (2) which depend on k_s (m), the roughness height to be calibrated, associated to the chosen closure relationship (e.g. Nikuradse law [11] for considering the low water depths face with grain size when tidal flats occurred (3)).

$$\begin{cases} \left(F_x^f, F_y^f\right) = g \, \dfrac{\boldsymbol{u}|\boldsymbol{u}|}{hC^2} \\ C^2 = \dfrac{2g}{C_F} \end{cases} \quad (2)$$

$$C = \frac{\sqrt{g}}{\kappa} \ln\left(\frac{12h}{k_s}\right) \quad (3)$$

where κ is the Von Kármán constant (0.4 for clear water), and $C_F = f(k_s)$ is the resulting friction coefficient.

ν_t (m²/s) is the diffusion coefficient which includes both the effects of molecular viscosity and of turbulence; it can be set to a constant value (in such a case it has to be calibrated), or depends on a closure model for turbulence (e.g. $\nu_t = f(k, \varepsilon)$ with k and ε, the turbulent kinetic energy and the turbulent dissipation respectively, two news unknowns that bring in addition two transport equations to solve).

IV. APIs : OPTIMIZATION BASED ON DATA ASSIMILATION

The APIs of TELEMAC-MASCARET SYSTEM (Fortan) make possible to have control on a simulation while running a case. Thus, some parameters (e.g. friction coefficient) can be manipulated during the simulation. The Python module TelApy gives access to the Fortan APIs and can be coupled in particular with other Python libraries dedicated to optimization [3].

In our study case, we focus on the automatic calibration based on a data assimilation algorithm of the ADAO library (https://pypi.org/project/adao/). The goal is to estimate the optimal parameters of the model by minimizing a cost function (4).

$$\begin{cases} J(X) = J_b + J_o \\ J_b = \frac{1}{2}(X - X_b)^T B^{-1}(X - X_b) \\ J_o = \frac{1}{2}\left(Y - H(X)\right)^T R^{-1}\left(Y - H(X)\right) \end{cases} \quad (4)$$

where $J(X)$ is the cost function – known as the variational data assimilation cost function 3D-VAR [12] – J_b and J_o are the background and observation components respectively; X is the vector of the parameters to be estimated; X_b represents the prior knowledge of X; Y is the observation vector and $H(X)$ is the result of the hydraulic solver that correspond to the observation vector; B and R are the background and observation error covariance matrices respectively. The resolution of the minimization problem is based on a gradient descent method, so-called constrained Broyden Fletcher Goldfarb Shanno Quasi-Newton method (c-BFGS-QN) [4]. The partial derivatives of hydraulic solver $H(X)$ are approximated by a classical finite difference method.

V. CALIBRATION AND VALIDATION STRATEGY

In this stage, we are interested only in the calibration of the hydrodynamic modelling. The simulations run with a fixed bottom, without tracer. Two parameters have to be calibrated: (i) the roughness height – flow resistance – that appears in the Nikuradse closure relationship; (ii) the diffusion coefficient – effective eddy viscosity – which depends on the chosen turbulence model. We start by the roughness height because, here, it plays a major role in comparison with the diffusion coefficient.

A. Calibration of the roughness height

First, we assume that there is no turbulence, with a constant viscosity model and a velocity diffusion coefficient set in first approximation. Its value differs from the molecular viscosity of water (10^{-6} m²/s) because it also includes the effects of turbulent viscosity. The value of the effective eddy viscosity was estimated with the turbulent boundary layer theory, whose the depth-mean value (5) was considered as a proper order of magnitude in shallow regime [13].

$$\nu_t \approx \kappa \sqrt{C_F} U H / 6 \quad (5)$$

The simulations are performed at steady flow condition that corresponds to the date of the bathymetric survey before the flushing event (Fig. 3, Tab. 1).

| Date
bathymetry before the flushing event	22/03/2018
Q (m³/s)	67
Downstream free surface elevation (m)	287.91
k_s (m) / equivalent $K_{Strickler}$ (m$^{1/3}$/s)
main stream	0.07 [0.01-0.1] / 40 [38-56]
k_s (m) / equivalent $K_{Strickler}$ (m$^{1/3}$/s)
vegetated area	25 [1-35] / 15 [14-26]
ν_t (m²/s)	0.008

Table 1. Value of the hydraulic boundary conditions and of the prior knowledge of the parameters to calibrate.

For that stage, we use the APIs detailed in section IV. The vector of parameters to estimate X is of length two and corresponds to the roughness heights of the main stream area and of the vegetated bank area (X could have included in addition the diffusion coefficient). The prior knowledge of X, named X_b, is estimated from the varying surface grain size measurements ($\sim 3D_{50}$ or again D_{90} – Fig. 6) for the main stream, and from an approximation valid for the vegetated area (height of the highest trees of the ripisylve, as willows or

poplars). One can notice that the bathymetric surveys are carried out at low flow, and as a consequence, the vegetated banks are unlikely to be flooded and the roughness height of the vegetated area would have little effect on the simulation. Finally, the observation vector Y corresponds to the free surface level records at the location of the 2 piezometers upstream and downstream the Fréterive gravel bar for that date (Fig. 7).
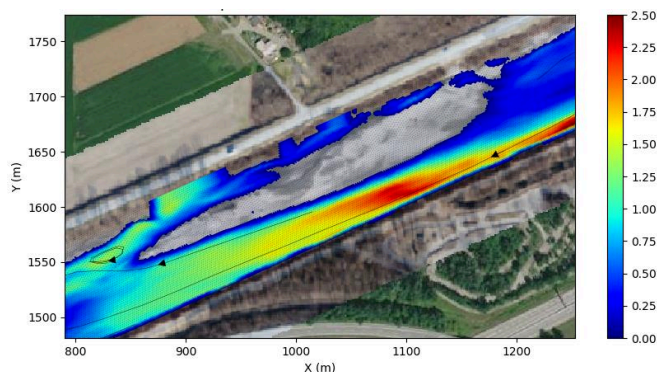
An example of simulation result is shown on Fig. 8.

Figure 8. Preliminary result of hydrodynamic simulation. Water depth (m) and streamlines in the interest area (22/03/2018, Q=67m³/s). The nodes where the water depth is below 0.05m are masked. Aerial photography (09/02/2018, Q=71 m³/s).

B. Validation

In order to validate the calibration of the roughness height, a new simulation is performed with unsteady flow conditions corresponding to the flushing event and the bathymetry before the flushing event. The free surface level records at the location of the piezometers are compared to the hydraulic solver results. Differences can be expected during the period of intense bedload transport, where the bottom changes.

A second validation stage consists in performing new simulations with the bathymetry surveyed after the flushing event and the steady flow conditions corresponding to the dates of aerial photography surveys. The aim is to ensure that the flooded surfaces are correctly reproduced by the model.

C. Choice of the turbulence model

Once the roughness heights calibrated and validated, the objective is to choose the best turbulence model and so diffusion coefficient to reproduce the size and the location of the recirculation zones using the velocities fields assessed by aDcp and LSPIV.

To do so, new simulations are performed with the post-flushing bathymetry and the steady flow conditions corresponding to the dates of the aDcp and LSPIV surveys (Fig. 3). Varying diffusion coefficient parameters are tested with the constant viscosity model. In addition, the other friction models implemented in TELEMAC-2D are tested (k-ε, mixing length, Smagorinski).

VI. CONCLUSION AND PERSPECTIVES

The calibration and validation of the 2D hydrodynamic model only involves two parameters related to the flow resistance and the eddy viscosity. The calculation requires measurements of bathymetry, water discharge and downstream free surface elevation, while the calibration and validation may be based on free surface elevation and current velocities. In addition, the grain size characterization is useful to have a first approximation of the friction coefficient, and so of the diffusion coefficient. The objective is to adjust these physical parameters until the comparison with the data is as accurate as possible. This can be time consuming and subjective, so automatic calibration trough the APIs is as well as relevant that it allows the consideration of many measurements while assessing simultaneously several parameters.

In the next stage, considering in addition the morphodynamic processes, with bedload, suspended sand, and cohesive suspended load strongly increases the number of parameters to estimate, as well as the data required. These information - sediment load and grain size for each class of sediment considered, settling velocities, erosion rate, critical shear stresses etc. - come with uncertainties that we must also considered. Considering the complexity of morphodynamic modelling (bed evolution, the numerous involved processes and their interactions), it is important to proceed step by step. The APIs and in particular data assimilation but also uncertainty quantification open new perspectives towards a better modelling.

REFERENCES

[1] A. J. Serlet, A. M. Gurnell, G. Zolezzi, G. Wharton, P. Belleudy, and C. Jourdain, 'Biomorphodynamics of alternate bars in a channelized, regulated river: an integrated historical and modelling analysis', *Earth Surface Processes and Landforms*, vol. 43, no. 9, pp. 1739–1756, Jul. 2018.

[2] Y. Audouin, T. Benson, M. De Linares, J. Fontaine, B. Glander, N. Huybrechts, R. Kopmann, A. Leroy, S. Pavan, C.-T. Pham, F. Taccone, P. Tassi, and R. Walther, 'Introducing GAIA, the brand new sediment transport module of the TELEMAC-MASCARET system', presented at the XXVIth TELEMAC - MASCARET Technical User Conference, Toulouse, France, 2019.

[3] Y. Audouin, C. Goeury, F. Zaoui, R. Ata, S. El Idrissi Essebtey, A. Torossian, and D. Rouge, 'Interoperability application of TELEMAC-MASCARET System', presented at the XXIIth TELEMAC - MASCARET Technical User Conference, Graz University of Technology, Austria, 2017.

[4] C. Goeury, A. Ponçot, J. P. Argaud, F. Zaoui, R. Ata, and Y. Audouin, 'Optimal calibration of TELEMAC - 2D models based on a data assimilation algorithm', presented at the XXIIth TELEMAC - MASCARET Technical User Conference, Graz University of Technology, Austria, 2017.

[5] T. Geay, S. Zanker, A. Hauet, C. Misset, and A. Recking, 'An estimate of bedload discharge in rivers with passive acoustic measurements: Towards a generalized calibration curve?', *E3S Web of Conferences*, vol. 40, p. 04009, 2018.

[6] V. Wendling, N. Gratiot, C. Legout, I. G. Droppo, C. Coulaud, and B. Mercier, 'Using an optical settling column to assess suspension characteristics within the free, flocculation, and hindered settling regimes', *Journal of Soils and Sediments*, vol. 15, no. 9, pp. 1991–2003, Sep. 2015.

[7] C. Legout, I. G. Droppo, J. Coutaz, C. Bel, and M. Jodeau, 'Assessment of erosion and settling properties of fine sediments stored in cobble bed rivers: the Arc and Isère alpine rivers before and after reservoir flushing', *Earth Surface Processes and Landforms*, vol. 43, no. 6, pp. 1295–1309, 2018.

[8] J. Le Coz, M. Jodeau, A. Hauet, B. Marchand, and R. Le Boursicaud, 'Image-based velocity and discharge measurements in field and laboratory river engineering studies using the free FUDAA-LSPIV software', in *Proceedings of the International Conference on Fluvial Hydraulics*, Lausanne, Switzerland, 2014.

[9] J. Hervouet, *Hydrodynamics of Free Surface Flows: Modelling with the finite element method*. 2007.

[10] C. Villaret, J.-M. Hervouet, R. Kopmann, U. Merkel, and A. G. Davies, 'Morphodynamic modeling using the Telemac finite-element system', *Computers & Geosciences*, vol. 53, pp. 105–113, Apr. 2013.

[11] J. Nikuradse, 'Laws of flow in rough pipes', Washington: National Advisory Committee for Aeronautics, 1950.

[12] J.-P. Argaud, 'User Documentation, in the SALOME 7.5 platform, of the ADAO module for Data Assimilation and Optimization'. EDF R&D report, 2016.

[13] C. A. Vionnet, P. A. Tassi, and J. P. Martín Vide, 'Estimates of flow resistance and eddy viscosity coefficients for 2D modelling on vegetated floodplains', *Hydrological Processes*, vol. 18, no. 15, pp. 2907–2926, Oct. 2004.